Title: TLR7-driven lupus autoimmunity induces hypertension and vascular alterations in mice.

Short title: TLR7 activation promotes vascular damage.

Authors: Iñaki ROBLES-VERA[a,*], Néstor DE LA VISITACIÓN[a,*], Marta TORAL[a], Manuel SÁNCHEZ[a,b], Manuel GÓMEZ-GUZMÁN[a,b], Francisco O'VALLE[b,c], Rosario JIMÉNEZ[a,b], Juan DUARTE[a,b,d], Miguel ROMERO[a,b]

[a] Department of Pharmacology, School of Pharmacy, University of Granada, CIBER-Enfermedades Cardiovasculares (CiberCV), Granada, Spain.

[b] Instituto de Investigación Biosanitaria de Granada (ibs.GRANADA), Granada, Spain

[c] Department of Pathological Anatomy, School of Medicine, University of Granada, Granada, Spain.

[d] Centro de Investigaciones Biomédicas (CIBM), Granada. Spain.

* I.R.-V and N.d.l.V. contributed equally as first author

Conflicts of Interest and Source of Funding:

The authors of this manuscript declare no conflicts of interest. This work was financially supported Grants from Comisión Interministerial de Ciencia y Tecnología, Ministerio de Economía y Competitividad (SAF2017-84894-R, SAF2014-55523-R), Junta de Andalucía (Proyecto de excelencia P12-CTS-2722 and CTS-164), Campus de Excelencia Internacional BIOTIC Granada (BS40-

2015) with funds from the European Union, and by the Ministerio de Economía y Competitividad, Instituto de Salud Carlos III (CIBER-CV), Spain. M.T. is a postdoctoral fellow of CIBER-CV. I.R.-V. is a predoctoral fellow of MINECO. N.d.l.V. is a predoctoral fellow of University of Granada. The cost of this publication was paid in part with FEDER funds.

Corresponding author: Juan Duarte. Department of Pharmacology, School of Pharmacy, University of Granada, 18071 Granada, Spain. Tel: (+34)-958241791, Fax: (+34)-958248264, Email: jmduarte@ugr.es

Word count: 7489

Number of tables: 1

Number of figures: 7

Number of Supplementary data: 8

Abstract

Objective: A critical role of TLR7 activation in accelerator lupus-like autoimmune disease initiation has been recently demonstrated. The aim of this study was to investigate whether TLR7 activation promotes increased blood pressure and vascular damage in wild-type mice treated with imiquimod.

Methods: Seven-nine week-old female BALB/c mice were randomly assigned to 2 experimental groups: control untreated and topically treated with imiquimod three times weekly for 4 or 8 weeks. Blood pressure, plasma anti-dsDNA autoantibodies and cytokines, spleen lymphocyte populations, vascular remodeling, endothelial function, and proinflammatory cytokines and oxidative stress levels were measured in all experimental groups.

Results: TLR7 activation leads to a gradual increase in blood pressure (≈ 20 mmHg at the end of the treatment), which is likely associated to elevated plasma levels of anti-dsDNA autoantibodies, splenomegaly, hepatomegaly, and severe expansion of splenic immune cells with an imbalance between pro-inflammatory T cells and regulatory T cells. Moreover, TLR7 activation also induces a marked vascular remodeling in resistance arteries as result of increased media-lumen ratio (≈ 40%), and impaired endothelium-dependent vasorelaxation in aortae from wild-type mice after 8 weeks of treatment. In addition, increased ROS production, as results of NADPH oxidase subunits up-regulation and enhanced vascular inflammation, were observed in aortae from IMQ-treated mice.

Conclusion: Our results demonstrate for the first time that TLR7 activation induced the development of hypertension and vascular damage in BALB/c

mice, and further underscore the increased vascular inflammation and oxidative stress as key contributing factors to cardiovascular complications in this TLR7-driven lupus autoimmunity model.

Key Words: vascular remodeling, endothelial dysfunction, hypertension, systemic lupus erythematosus, TLR7 activation.

Abbreviations: SLE, systemic lupus erythematosus; TLRs, Toll-like receptors; TLR7, Toll-like receptor 7; TLR9, Toll-like receptor 9; IMQ, imiquimod; IFN, type I interferons; SBP, systolic blood pressure; MABP, mean arterial blood pressure; HR, heart rate; anti-dsDNA, plasma anti-double-stranded; ACh, acetylcholine; O_2^-, superoxide anions; NO, nitric oxide; eNOS, endothelial NO synthase; L-NAME, N(ω)-nitro-L-arginine methyl ester; NADPH, nicotinamide adenine dinucleotide phosphate; Apo, apocynin; SNP, sodium nitroprusside; DHE, dihydroethidium; DAPI, 4,6-diamidino-2-phenylindoledichlorohydrate; RLU, relative luminescence units; MT, MCSA, media cross-sectional area; M/L media-lumen ratio; RT-PCR, reverse transcriptase-polymerase chain reaction, VCAM-1, vascular cell adhesion molecule-1.

INTRODUCTION

Systemic lupus erythematosus (SLE) is a heterogeneous systemic autoimmune disease characterized by innate and adaptive immune responses dysregulation with a loss of tolerance to nuclear self-antigens, an anomalous production of proinflammatory cytokines and multiorgan damage (1). SLE is associated with an increased prevalence of renal and cardiovascular diseases, which are major causes of mortality in these patients, even after correction of the traditional risk factors (2, 3). Hypertension is a well-recognized risk factor for cardiovascular disease development in SLE, as evidenced by its contribution in acceleration of atherosclerosis and arterial stiffening (4, 5). In addition, numerous studies suggest direct detrimental effects on the endothelium during SLE, beyond the concomitance with traditional cardiovascular risk factors, including obesity, hypertension, dyslipidemia and diabetes mellitus (6-8). Vascular inflammation and inflammatory cells infiltration are known to contribute to the pathogenesis of endothelial dysfunction in SLE, largely driven by immune dysregulation (9, 10). Despite the high incidence of hypertension and vascular dysfunction in SLE patients, there are few studies directed at understanding the mechanisms of hypertension and endothelial dysfunction during SLE, due to the diversity in patient populations, severity of SLE and therapeutic strategies used to treat SLE (11, 12). Currently available data regarding the pathophysiological mechanisms that promote the development of hypertension during SLE have focused on female NZBWF1 mice, a genetic mouse model of lupus nephritis accompanying with hypertension that develop similar features to human SLE (13-15). However, these studies have limited utility for examining mechanisms

of SLE hypertension and the possible role of altered vascular function in the progression of SLE.

Toll-like receptors (TLRs) are a family of innate pattern recognition receptors that recognize a wide range of pathogen-associated molecular patterns (PAMPs) and initiate innate immune responses (16). Accumulating evidence supports the pathological role of TLRs signaling dysfunction in the induction and development of human and spontaneous murine models of SLE (17, 18). Specifically, several recent studies have suggested that activation of endosomal TLR7 or TLR9 on dendritic cells and B lymphocytes is a critical step for lupus disease development in both humans and murine models, through the induction of type I interferons (IFN) and other proinflammatory cytokines (19, 20). However, an opposing relationship between TLR7 and TLR9 has been suggested as a potential mechanism regulating autoimmunity in SLE. Thus, TLR7 activation has proven to be a key critical in accelerator lupus disease initiation, while TLR9 plays a protective role in lupus-associated autoimmunity (21, 22).

Recently, a lupus model induced by epicutaneous application of TLR7 agonist imiquimod (IMQ) has been described in several genetic backgrounds, including BALB/c mice (23). TLR7 activation leads to several phenotypic and functional changes characteristic of human SLE, including elevated levels of autoantibodies and multiple organ involvement (23). Although several studies have used TLR7 transgenic (TLR7tg) lupus-prone mice to elucidate the pathogenesis of SLE (24, 25), these genetically modified lupus models have drawbacks because of their polygenic (disease is driven by multiple alleles,

such as B6.RIIB(-/-)/yaa mice) or monoallelic nature (disease is driven by single alleles, such as B6. Yaa), thereby adding additional confounding factors to the effect of TLR7 activation alone. To date, there have not been studies that evaluate changes in blood pressure in murine lupus-induced by TLR7 activation and nor studies to directly assess whether alterations in vascular structure and function may to contribute to raised blood pressure during lupus disease progression in this model. Therefore, the aim of the present study was to examine whether chronic topical application of IMQ in wild-type female BALB/c mice promotes increased blood pressure and analyze whether these changes in blood pressure are associated with vascular alterations.

METHODS

Animals and Experimental Groups

Seven-nine week-old female BALB/c mice obtained from JANVIER (Le Genest, France), were randomly assigned to two experimental groups of 8-10 animals each: control untreated (Ctrl) and treated with Imiquimod (IMQ) for 4 or 8 weeks. IMQ-treated mice receive three times weekly topical treatment on their right ears with 1,25 mg of 5% imiquimod cream (Aldara®) from Laboratories MEDA PHARMA SALU (Madrid, Spain). Animals were maintained at a constant temperature (24º ± 1) with a 12-hour light/dark cycle in a specific pathogen-free environment and were provided with water and standard laboratory diet (SAFE A04, Augy, France) ad libitum.

All experimental protocols to carry out in this study were conformed to the National Institutes of Health Guide for the Care and Use of Laboratory

Animal and were approved by the Animal Care and Ethics Committee of the University of Granada (Spain; reference number: 68-CEEA-OH-2015).

Morphological variables

Body weight of mice was measured at the beginning and end of treatment. The heart, kidney, spleen and liver were collected and weighted. Then, the atria and the right ventricle were then removed and the remaining left ventricle was also weighed. Finally, the cardiac, left ventricular, renal, splenic and hepatic weight indices were calculated by dividing the weight of each organ by the tibia length. All tissue samples were frozen in liquid nitrogen and then stored at -80ºC.

Blood pressure measurements

Systolic blood pressure (SBP) was measured each two weeks at room temperature using tail-cuff plethysmography as described previously . At the end of the experimental period, mean arterial blood pressure (MABP) and heart rate (HR) were measured by intra-arterial register in conscious mice and unrestrained conditions by continuously recorded (MacLab; AD Instruments, Hastings, UK). MABP and HR values obtained during the last 30 min were averaged for intergroup comparisons(14).

Vascular reactivity studies

Descending thoracic aortic rings were mounted in a wire myograph (model 610M, Danish Myo Technology, Aarhus, Denmark) for isometric tension

measurement as previously described (15). The organ chamber was filled with Krebs solution (composition in mM: NaCl 118, KCl 4.75, $NaHCO_3$ 25, $MgSO_4$ 1.2, $CaCl_2$ 2, KH_2PO_4 1.2 and glucose 11) at 37 ºC and gassed with 95% O_2 and 5% CO_2 (pH 7.4). On basis of length–tension characteristics obtained via the myograph software (Myodaq 2.01), aorta arteries were maintained at a resting tension of 0.5 g.

Endothelium-dependent relaxation curves to acetylcholine (Ach, 1nM - 10µM) were performed in intact rings pre-contracted by the thromboxane A_2 analog U46619 (10 nM) in the absence or in the presence of the endothelial nitric oxide (NO) synthase (eNOS) inhibitor N(ω)-nitro-L-arginine methyl ester (L-NAME, 100 µM), or the non-selective nicotinamide adenine dinucleotide phosphate (NADPH) oxidase inhibitor apocynin (Apo, 10 µM) both added 30 min before of U46619. In another experimental set, endothelium-independent relaxant responses to sodium nitroprusside (SNP, 0.1nM–1 µM) were studied in the dark in endothelium-denuded vessels pre-contracted by U46619 (10 nM). Relaxant responses to Ach and SNP were expressed as a percentage of pre-contraction induced by U46619.

In situ detection of vascular reactive oxygen species levels and NADPH oxidase activity

Ex vivo vascular reactive oxygen species (ROS) content were measured by the oxidative fluorescent dye dihydroethidium (DHE) in aortic segments as previously described (14). Briefly, unfixed thoracic aortic rings were cryopreserved (0.1 M PBS plus 30% sucrose for 1-2 h), included in optimum cutting temperature

compound medium (Tissue-Tek; Sakura Finetechnical, Tokyo, Japan) and frozen (-80 ºC) until their use. 10 µm cross-sections were obtained in a cryostat (Microm International Model HM500 OM) and incubated for 30 min in HEPES buffer solution, containing DHE (10 µM), counterstained with the nuclear stain 4,6-diamidino-2-phenylindoledichlorohydrate (DAPI, 30 nM). In the following 24 h, sections were examined on a fluorescence microscope (Leica DM IRB, Wetzlar, Germany) and photographed. Ethidium and DAPI fluorescence were quantified using ImageJ (version 1.32j, NIH, http://rsb.info.nih/ij/) and ROS production was estimated from the ratio of ethidium/DAPI fluorescence.

NADPH oxidase activity in intact aortic rings was determined using the lucigenin-enhanced chemiluminescence assay as previously described (14). Concisely, aortic rings from all experimental groups were incubated for 30 minutes at 37 °C in HEPES containing a physiological salt solution (pH 7.4) with the following composition (in mM): NaCl 119, HEPES 20, KCl 4.6, $MgSO_4$ 1, Na_2HPO_4 0.15, KH_2PO_4 0.4, $NaHCO_3$ 1, $CaCl_2$ 1.2 and glucose 5.5. Then, rings were then placed in tubes containing the physiological salt solution, with or without NADPH (100 µM) to stimulate aortic production of superoxide anions (O_2^-) and lucigenin was injected automatically at a final concentration of 5 µM. NADPH oxidase activity was determined by measuring luminescence over 200 s in a scintillation counter (Lumat LB 9507, Berthold, Germany) in 5 s intervals and calculated by subtracting the basal values from those in the absence of NADPH. The vessels were then dried, and the dry weight was determined. NADPH oxidase activity was expressed as relative luminescence units (RLU) per min per mg dry aortic tissue. In another set of experiments, the NADPH stimulated ROS

production in homogenates from mesenteric arteries was also measured by DHE fluorescence assay in the microplate reader, as described previously (26).

Histopathological analysis

Kidney and superior mesenteric artery sections was obtained from each mouse by dissection and immersed in free-calcium Krebs solution for 30 min. Then, samples were fixed in 10% buffered formalin for 24 hours, dehydrated in graded ethanol solutions and embedded in paraffin.

For each artery, a series of four 5 μm cross sections were made on a precision microtome (Microm International Model HM500 OM) and stained with hematoxylin-eosin to highlight structure of vascular wall. Arterial media thickness (MT), lumen diameter (LD), media cross-sectional area (MCSA) and media-lumen ratio (M/L) were measured, as previously described (27), using a computer equipped with a Leica Q500MC image analyser connected to a video camera of a Leica Leitz DMRB microscope (Leica, Wetzlar, Germany). However, for the evaluation of kidney histopathology, 4 μm sections were cut along the central axis of the biopsies. Then, samples were dewaxed and rehydrated for staining with hematoxylin-eosin, periodic acid-Schiff, and Masson's trichrome. Morphological study on light microscopy was done in a blinded fashion (MR and FO) and the presence of SLE-like lesions was studied. Glomerular cellularity (proliferation) was evaluated by counting the number of nuclei per glomerular cross-section (20 glomerular cross-sections per mouse) (28). We considered proliferative glomeruli when the number of cells were >30.

Renal injury evaluation

Renal injury was assessed by protein determination from urine samples collected for 24 hours (29). For that, mice were housed in metabolic cages at the end of the experimental period to collect urine samples. Proteinuria was determined using bovine serum albumin as standard and the results were expressed as mg of protein excreted, normalized by body weight (per 100 g of mice), and time (during 24 h). The means of the values obtained during the 2 experimental days were used for statistical analysis between groups.

Plasma determinations

Blood samples were cooled in ice and centrifuged for 10 min at 3,500 rpm at 4 ºC, and the plasma frozen at -80 °C. Plasma anti-double-stranded (anti-dsDNA) autoantibodies and IFNα levels were determined by a commercial ELISA according to the manufacturer's instructions (Alpha Diagnostic International, San Antonio, TX, and Thermo Fisher Scientific, Madrid, Spain, respectively). Plasma cytokines were measured by a multiplex assay using Luminex ™ xMAP technology (Thermo Fisher Scientific, Madrid, Spain).

Flow Cytometry

Spleens were collected from all groups. The tissues were smashed with wet slides very well to decrease friction and then the solutions were filtered through a 70 µm cell strainer. Cells were isolated followed by lysis of red blood cells with Gey's solution. 10^6 cells were counted and blocked with anti-CD3 (clone17A2, eBioscience) and anti-CD28 (clone 37.51, eBioscience) for 30

minutes at 37°C to avoid non-specific binding to Fc-gamma receptors. After 4 hours, cells incubated with a protein transport inhibitor (BD GolgiPlugTM) for an optimum detection of intracellular cytokines by flow cytometry. Then, the cells were transferred to polystyrene tubes for the surface staining with mAbs anti-CD4 (PerCP-CyTM, clone RM4-5 BD PharmigenTM), anti-B220 (APC, clone RA3-6B2, BD PharmigenTM) and viability dye (LIVE/DIED® Fixable Aqua Dead cell Sain Kit, Molecular Probes, Oregon, USA) for 20 min at 4°C in the dark. The lymphocytes were then fixed, permeabilized with the Fix/Perm Fixation/Permeabilization kit (eBioscience, San Diego, USA) and intracellular staining was achieved with mAbs anti-Foxp3 (PE,clone FJK-16s, eBioscience, San Diego, USA), anti-IL-17A (PE-Cy7, clone eBio17B7, eBioscience, San Diego, USA) and anti-lFNγ (Alexa Fluor® 647, DB-1, 6B2 BD PharmigenTM, New Jersey, USA) for 30 min at 4°C in the dark. All samples were analyzed using a flow cytometer CANTO II (BD Biosciences) with FlowJo software (Tree Star, Ashland, OR, USA) (15).

Gene expression analysis

The analysis of gene expression in aorta and mesenteric arteries were performed by reverse transcriptase-polymerase chain reaction (RT-PCR) analysis, as previously described (14, 30). For this purpose, total RNA was extracted by homogenization using TRI Reagent® following the manufacturer's protocol. All RNA samples were quantified with the Thermo Scientific NanoDropTM 2000 Spectrophotometer (Thermo Fisher Scientific, Madrid, Spain) and 2 µg of RNA were reverse transcribed using oligo(dT) primers (Promega, Southampton, UK).

Polymerase chain reaction was performed with a Techne Techgene thermocycler (Techne, Cambridge, UK). The sequences of the sense and antisense primers used for amplification are described in **Table S1.** The efficiency of the PCR reaction was determined using a dilution series of standard vascular samples. To normalize mRNA expression, the expression of the housekeeping genes GAPDH and RPL13 were used. The mRNA relative quantification was calculated using the ΔΔCt method.

Western blotting analysis

40 µg of protein per lane from aortic homogenates were run on a sodium dodecyl sulphate (SDS)-polyacrilamide electrophoresis. Then, proteins were transferred to polyvinylidene difluoride membranes (PVDF), incubated with primary mouse monoclonal anti-eNOS antibody (Transduction Laboratories, San Diego, California, USA) overnight and with the correspondent secondary peroxidase conjugated antibody. Antibody binding was detected by an ECL system (Amersham Pharmacia Biotech, Amersham, UK) and densitometric analysis was performed using Scion Image-Release Beta 4.02 software (http://www.scioncorp.com) as described (14, 30). Samples were re-probed for expression of smooth muscle α-actin.

Reagents

All chemicals were obtained from Sigma-Aldrich (Barcelona, Spain), unless otherwise stated.

Statistical analysis

Results are expressed as means ± SEM of measurements. The evolution of tail SBP over time was compared using the nested design, with treatment and weeks as fixed factors and the mouse as random factor. When the overall difference was significant, comparisons were made using Bonferroni´s method with an appropriate error. Analysis of the nested design was also carried out with groups and concentrations to compare the concentration-response curves to acetylcholine. The remaining variables were tested on normal distribution using Shapiro-Wilk normality test and compared using one-way ANOVA and Tukey post hoc test. Differences of at least $P<0.05$ were considered statistically significant. Statistical analysis was carried out using Graph Pad Prism 7 software.

RESULTS

Blood pressure, target organs damage and systemic inflammation are increased in Lupus-induced by TLR7 activation.

BALB/c mice exposed to IMQ showed high incidence of death rate (approximately 20%, **Fig. 1A)** and profound weight gain compared with control animals (final weight: 24.10 ± 0.62 g and 21.89 ± 0.54, respectively, $p<0.05$) at 8 weeks of treatment, as previously reported in the original description of this model (23). The gonadal and mesenteric fat weight indices were reduced in IMQ-treated mice **(Table 1)** in spite of the weight gain observed which appears to be related to the development of edema and swelling instead. IMQ-treated mice also displayed a progressive increase in SBP **(Fig. 1B)**, and in the final mean arterial blood pressure **(Fig. 1C)** as measured by tail-cuff

plethysmography and direct recordings, respectively, being approximately 20 mmHg higher than in control mice at the end of the experiment. No significant changes in heart rate were induced by IMQ treatment (**Fig. 1D)**. In addition, both heart weight/tibia length and left ventricular weight/tibia length were higher in IMQ-treated mice than in control mice at 8 weeks **(Table 1)**, whereas renal hypertrophy and hepatomegaly were displayed from 4 weeks of IMQ treatment **(Table 1)**.

The IMQ-induced lupus model is characterized by renal injury associated with increased plasma levels of autoantibodies in wild-type mice (22, 23). As expected, we found significant higher plasma levels of anti-dsDNA autoantibodies (**Fig 2A)** and renal injury (**Fig. Suppl. 1)** in IMQ-treated mice compared with control mice. We also found a marked splenomegaly in IMQ-treated mice (**Fig 2B)**, which was associated with autoimmune disease progression. In addition, a reduced clearance of apoptotic cells is associated with progressive lupus-like autoimmune disease and increased production of autoantibodies (31, 32). Opsonins, such as C1q, thrombospondin-1 and milk fat globule-epidermal growth factor-8, are proteins released by macrophages that enhance the recognition and phagocytosis of apoptotic cells by macrophages. The primary source of circulating opsonins in the serum is the liver resident macrophages, Kupffer cells (33). This prompted us to investigate the opsonin expression in the livers of mice from all experimental groups. We found that activation of TLR7 by topically administration of IMQ reduced hepatic opsonins gene expression only in IMQ-treated mice as compared with control mice only after 8 weeks of treatment (**Fig. 2C)**.

Finally, we evaluate the immunomodulatory actions of TLR7 activation by measuring the number of total cells and the levels of B and T cells in spleens from all experimental groups. IMQ treatment led to increase in splenocyte numbers and in the percentages of both splenic B cells and T cells from 4 weeks of IMQ treatment as compared with the control group **(Fig. 3A-C).** Specifically, the percentages of Th1 and Th17 cells were significantly increased only at 8 weeks of treatment, whereas percentage of Treg cells was reduced in splenocytes from all experimental groups **(Fig. 3D-F)**. Representative flow cytometry of spleens are shown in the supplemental data (**Fig. Suppl. 2)**. Besides, plasma levels of IFN-α, IFN-γ, IL-21, TNF-α, IL-6, and IL-17 were also increased in IMQ-treated mice at 8 weeks when compared with control (**Fig. Suppl. 3)**. Taken together, these results suggest that TLR7 activation by topical application of IMQ resulted in systemic inflammation at 8 weeks of treatment, being these results in concordance with previously described (22, 23, 34).

Lupus-induced by TLR7 activation promotes vascular remodeling and endothelial dysfunction.

Structural alterations in resistance arteries may be considered an important contributing factor to the pathogenesis of hypertension in humans and animal models (35, 36). Here, we found that topically administration of IMQ is associated with structural alterations in superior mesenteric arteries characterized by a significant smaller lumen diameter and increase in the media thickness and media-lumen ratio (M/L) (≈ 40%) in BALB/c mice after 8 weeks (**Fig. 4A-D**). We also found a small, but not significant, increase in the media

cross-sectional area (MCSA) (≈ 11%) in these resistant arteries from IMQ-treated mice (**Fig. 4E**). However, no significant changes were observed at 4 weeks of treatment.

Similarly, SLE hypertension is known to associate with an impaired vascular function (13, 15, 37). For that reason, we determine whether endothelial-dependent relaxation and contraction are altered in this model. We observed that aorta from IMQ-treated mice showed strongly reduced endothelium-dependent vasodilator responses to ACh only after 8 weeks of topical treatment (maximal effect, 60.35 ± 2.69% versus 79.34 ± 1.79% in the control group; P<0.001) (**Fig. 5A**). The incubation for 30 minutes with the eNOS inhibitor L-NAME abolished the relaxant response induced by ACh in all experimental groups, involving NO in this relaxation (**Fig. 5B**). Moreover, no differences were observed in the endothelium-independent relaxant response to the NO donor sodium nitroprusside in aortic rings from both control and IMQ-treated groups, excluding changes in the sensitivity of the NO-cGMP pathway in vascular smooth muscle cells (**Fig. 5C**). In addition to examining endothelial-dependent relaxation, we also tested whether there are changes in vessel contractility that might contribute to endothelial dysfunction. No differences were found among all experimental groups in the contractile response induced by U46619 in both intact aortic rings and in the presence of L-NAME (**Table S2**). Besides, since endothelial-dependent relaxation was progressively impaired in IMQ-treated mice, we only evaluated whether eNOS expression was altered at 8 weeks of IMQ treatment. Aortic eNOS mRNA levels (**Fig. 5D**) and protein expression (**Fig. 5E**) were reduced in IMQ-treated mice.

Finally, we also found that these changes in vascular structure and function are associated with a marked increased vascular TLR7 mRNA expression in aortae and mesenteric arteries from IMQ-treated mice, while vascular TLR9 mRNA expression was unaffected (**Fig. Suppl. 4**).

Vascular oxidative stress and inflammation are increased in Lupus-induced by TLR7 activation.

Reactive oxygen species (ROS) , particularly O_2^-, play an important role in vascular tone and structure, contributing to pathological mechanisms related to endothelial dysfunction, arterial remodeling and vascular inflammation (38). Our results showed that aortic rings from IMQ-treated mice display marked increased red ethidium fluorescence staining in vascular wall when compared with control group (**Fig 6A**), suggesting an increased vascular ROS production. Moreover, the activity of the NADPH oxidase, considered the major source of O_2^- in the vascular wall, was also markedly increased in aorta from IMQ-treated mice at 8 weeks of treatment (**Fig. 6B**), which was correlated with significant mRNA increase of its catalytic subunits NOX2, $p22^{phox}$ and $p47^{phox}$ (**Fig 6C**). Likewise, to evaluate the role of NADPH oxidase-driven ROS production in the impaired relaxation to ACh in aorta from IMQ-treated mice, we analyzed the effects of the non-selective NADPH oxidase inhibitor apocynin in endothelium-dependent relaxation to ACh. No significant differences among groups were observed after incubation with apocynin, suggesting that an increased NADPH oxidase activity is involved, at least in part, in the endothelial dysfunction found in aorta from IMQ-treated mice (**Fig 6D**).

Additionally, in order to determine the role of NADPH oxidase-derived ROS on vascular remodeling we also measured the activity of the NADPH oxidase and the mRNA expression of its catalytic subunits in mesenteric arteries. A significant increased NADPH oxidase activity and NOX2, $p22^{phox}$ and $p47^{phox}$ mRNA overexpression were found in mesenteric arteries homogenates from IMQ-treated mice as compared to the control group **(Fig. Suppl. 5)**. Incubation with PEG-SOD or Tiron for 30 min abolished this increased NADPH oxidase activity, involving O_2^- as main ROS that contribute to the vascular remodeling in these mice.

On the other hand, given the key role of proinflammatory cytokines and chemokines to contribute to the pathogenesis of vascular remodeling and endothelial dysfunction in SLE (9, 39), we also analyzed the transcript level of vascular adhesion molecules and proinflammatory cytokines in aorta and mesenteric arteries homogenates from control and IMQ-treated mice. Thus, we found a higher mRNA expression of vascular cell adhesion molecule-1 (VCAM-1) and proinflammatory cytokines IFN-α, IFNγ, IL1β, IL-6 and IL-17, while mRNA expression of IL-10 and TFG-β were reduced, in aorta (**Fig. 7**) and mesenteric artery **(Fig. Suppl. 6)** homogenates from IMQ-treated mice as compared to control mice. These results are correlated with increased systemic inflammation and changes in splenic lymphoid cell populations induced by IMQ described above.

DISCUSSION

We demonstrate, for the first time to our knowledge, that TLR7 activation

by epicutaneous application of IMQ results in a gradual increase in arterial blood pressure, which is likely associated to autoimmune disease progression as evidenced by elevated plasma levels of anti-dsDNA autoantibodies, splenomegaly and hepatomegaly, and severe expansion of splenic immune cells with enhancement of lymphocyte polarization to proinflammatory phenotype. Moreover, our present results show a marked hypertrophic effect in target organs for high blood pressure, such as heart and kidney. Additionally, and as a novel finding, the activation of TLR7 by IMQ also induces vascular remodeling in resistance arteries and endothelial dysfunction in aortae from wild-type mice that seem to be related to loss of NO bioavailability and increased ROS production, as results of NADPH oxidase subunits up-regulation and enhanced vascular inflammation.

Increasing evidence supports the idea that increased TLR7 activity on plasmacytoid dendritic cells (pDCs) and B lymphocytes plays a pathogenic role in the development of humans and murine models of SLE, through the induction of type I interferons (IFN) and other proinflammatory cytokines (40, 41). Recently, TLR7 activation by topical application of IMQ has shown to induce severe glomerulonephritis and renal injury associated with elevated autoantibodies generation (22, 23, 34). In our experiment, we also found increased plasma levels of anti-dsDNA autoantibodies in IMQ-treated mice, which are correlated with albuminuria and morphological alterations in renal cortex from these mice, which were significant after 4 weeks of IMQ treatment. Interestingly, our results showed a severe expansion of splenic immune cells in association with lymphocyte polarization to proinflammatory phenotype. Of note,

we observed an imbalance between T helper cell subtypes (Th1 and Th17) and regulatory T cells (Treg) in spleen from IMQ-treated mice, with a predominance of the former. These results are consistent with previous evidences showing that TLR7 activation by IMQ is associated to autoimmune disease progression because of a lymphoproliferative disorder as a result of abnormalities in B-cell activation and enhanced T helper-1 (Th1)-type immune responses, at least partially attributable to a defect in immunosuppressive Treg function (22, 42).

Furthermore, a defective clearance of apoptotic cells is also associated with progressive lupus-like autoimmune disease and increased production of autoantibodies (31, 32). Notably, an impaired ability to engulf apoptotic cells has been demonstrated in both C1q-deficient humans and mice, which was related to a higher risk to develop SLE (43, 44). Here, we found a reduced expression of hepatic opsonins only in IMQ-treated mice as compared with control mice, suggesting that the activation of TLR7 causes a deficiency in the clearance of apoptotic cells which together with the increased percentage of splenic B cells and plasma levels of IL-21, might contribute to the exacerbation of the anti-dsDNA autoantibodies observed in IMQ-treated mice, being these results in concordance with previously described (32, 45).

Previous studies have shown that autoimmune disease progression and the resultant increase of systemic inflammation and renal damage are important underlying factors involved in the development of hypertension and vascular dysfunction associated to SLE (2, 3, 46). In fact, it has been shown that preventing autoimmunity with immunosuppressive therapy attenuates lupus disease progression and protects against the development of hypertension (47,

48). Our results demonstrate for first time a progressive increase in arterial blood pressure induced by TLR7 activation in IMQ-treated mice, without changes in heart rate. Moreover, hypertensive IMQ-treated mice developed cardiac and renal hypertrophy when compared with control mice. However, currently available data do not allow establishing a direct relationship between glomerulonephritis and increased blood pressure in both murine models and patients with SLE (46, 49). Thus, MRL/lpr and BXSB mice, two commonly used murine models of SLE, develop lupus nephritis similar to that observed in human SLE, but not hypertension (50). In our study, we found that the increase in arterial blood pressure begins after the development of proteinuria, suggesting that early renal injury may contribute to the evolution of hypertension during lupus disease progression induced by TLR7 activation. These results are in agreement with observed in female NZBWF1 mice, a genetic mouse model of lupus nephritis accompanying with hypertension (13, 15).

Numerous studies suggest that the presence of vascular remodeling in resistance arteries and endothelial dysfunction are crucial in the pathogenesis of SLE hypertension in humans and animal models (13, 14, 37, 39). In this study, we found that TLR7 activation induced significant M/L ratio increase as a result of reduced lumen diameter and increased medial thickness in superior mesenteric arteries from IMQ-treated mice, observed only at 8 weeks of treatment. These structural alterations may be mediated by the influence not solely of hemodynamic load but additionally by the effect of oxidative stress, local growth factors and pro-inflammatory cytokines (51, 52). However, it is difficult to prove whether vascular remodeling contributes to, or is only related

to, the progression of hypertension with our results. Recently, Liu et al. (2018) have also found endothelial dysfunction triggered by IMQ treatment in wild-type mice (22). Importantly, we also demonstrate that IMQ-treated mice display significant impaired endothelium-dependent vasorelaxation compared with control mice. These results are clinically relevant due to endothelial dysfunction is highly prevalent in lupus patients and represents the earliest indicator of the development of lupus-related cardiovascular diseases (6-8). Endothelial dysfunction is characterized by impaired NO availability and concomitant increased reactive oxygen species (ROS) generation (53). It is well known that NO secretion is required for normal endothelium-dependent vasodilatation, and a deficiency of eNOS function in endothelial cells have been reported to happen in both murine models and humans with SLE (15, 54). We found that endothelium-dependent relaxations induced by ACh were abolished by eNOS inhibition with L-NAME, suggesting a defect in NO pathway in IMQ-treated mice. However, not significant changes in vasodilator response to the NO donor nitroprusside were observed in all experimental groups, suggesting that sensitivity to the NO-cGMP pathway in vascular smooth muscle cells was unaltered. Moreover, contractile response to U46619 was also unaffected in aorta from IMQ-treated mice as compared with control mice in both the absence and presence of L-NAME. Taken together, these results suggest that the impaired response to ACh in this model may be mediated mainly by reduced NO availability than by changes in the signaling of NO in vascular smooth muscle cells and changes in vessel contractility.

It is well established that vascular inflammation and inflammatory cells

infiltration are contributing factors to the pathogenesis of vascular dysfunction in SLE, largely driven by immune dysregulation (9, 10). Previous studies have shown that TLR7 activation causes an increase circulating proinflammatory cytokines in both wild-type and TLR9-deficient mice, which are potentially involved in the pathogenesis of lupus and its deleterious effects in the vasculature (22, 23). Accordingly, we also observe increased plasma levels of proinflammatory cytokines IFN-α, IFN-γ, IL-21, TNF-α, IL-6 and IL-17 in IMQ-treated mice, which was correlated with changes in lymphoid cell populations observed in the spleen from these mice. High concentrations of proinflammatory cytokines down-regulate eNOS bioactivity and increase oxidative stress (55, 56). Interestingly, we found a progressive reduced eNOS mRNA levels and protein expression in aorta from IMQ-treated mice. Although our study is limited due to the lack of direct NO release and eNOS activity measures, our results suggest that changes in eNOS expression might to, at least partially, contribute to the loss of NO production. In fact, a recent study have described that IFN-α negatively regulates the expression of eNOS and NO production in endothelial cells (57).

Oxidative stress is an important contributor to vascular remodeling and endothelial dysfunction associated to SLE, acting as mediator of the link between autoimmune responses and vascular inflammation (39, 56). Our results show an increased production of ROS in both aorta and mesenteric arteries from IMQ-treated mice which is correlated with significant NADPH oxidase activity as results of its catalytic subunits NOX2, $p22^{phox}$ and $p47^{phox}$ overexpression. This exacerbated NADPH oxidase-driven ROS production

seems to be a key event in the development of vascular structural alterations and endothelial dysfunction induced by TRL7 activation. Thus, incubation with the NADPH oxidase inhibitor apocynin increased the aortic endothelium-dependent relaxation to acetylcholine in IMQ-treated mice to similar level that found in control. Furthermore, NADPH oxidase-derived ROS may be a key component in upregulation of TLRs in the vasculature (58). Accordingly, our results show a marked increased vascular TLR7 mRNA expression in aortae from IMQ-treated mice, while vascular TLR9 mRNA expression was unaffected.

In addition, TLR7 activation by IMQ stimulates the release of proinflammatory cytokines and chemoattractant proteins increasing the expression of adhesion molecules and trigger plaque inflammation by recruiting both monocytes and T-lymphocytes, which have an impact on the development of premature atherosclerosis in SLE (59). Moreover, it has been recently described that IL-10 and TFG-β, two inhibitory cytokines, are able to synergistically regulate humoral immunity and improved pathological conditions in IMQ-induced lupus model by suppression of B cell activation induced by TLR7 stimulation (60). According to these previous results, we observe a marked increase in mRNA expression of vascular cell adhesion molecule-1 (VCAM-1) and proinflammatory cytokines IFN-α, IFNγ, IL-6, IL1β and IL-17 in aortic and mesenteric arteries homogenates from IMQ-treated mice, whereas mRNA expression of IL-10 and TFG-β are reduced. Postnatal smooth muscle cells-specific deletion of TGF-β type II receptor is reported to cause the rapid thickening of the thoracic aorta (61). Thus, reduced TFG-β mRNA levels found in mesenteric arteries from IMQ-treated mice might be involved in the structural

modification induced by TLR7 activation. Taken together, the detrimental vascular effects of TLR7 activation by IMQ might be the results of the increase in plasma cytokines and direct effects on the vasculature through increasing oxidative stress and vascular inflammation via an imbalance between pro-inflammatory and inhibitory cytokines.

In conclusion, our results demonstrate for the first time that TLR7 activation by chronic topical application of IMQ induced a progressive increase of blood pressure and vascular structural and functional changes in wild-type mice and suggest that this vascular damage may be an important mechanism contributing to hypertension during lupus disease induced by TLR7 activation. In addition, our results underscore the increased vascular inflammation and oxidative stress as key molecular mechanisms contributing to cardiovascular complications in this TLR7-driven lupus autoimmunity model. Therefore, our findings identify TLR7 as a promising target for an alternative approach in the treatment of SLE and its associated vascular damage. Now that our study has highlighted the potential importance of TLR7 signaling in SLE hypertension and vascular dysfunction, future studies should be performed to focus in TLR7 as a therapeutic target.

ACKNOWLEDGEMENTS

This research was supported by the Ministerio de Economía y Competitividad, Junta de Andalucía, Campus de Excelencia Internacional BIOTIC Granada, Instituto de Salud Carlos III and Universidad de Granada.

Authors' contributions

M.R. and J.D. participated in research design; M.R., I.R.-V., N.d.l.V., M.T., M.S., M.G.-G. and R.J. performed the most of experiments; F.O.; M.R. and J.D. performed Histopathological analysis; M.R., I.R.-V., N.d.l.V., M.T., R.J., and J.D. contributed to data analysis and interpretation. M.R. and J.D. wrote or contributed to the writing of the manuscript.

REFERENCES

1. Liu Z, Davidson A. Taming lupus-a new understanding of pathogenesis is leading to clinical advances. Nat Med. 2012;18(6):871-82.
2. Giannelou M, Mavragani CP. Cardiovascular disease in systemic lupus erythematosus: A comprehensive update. J Autoimmun. 2017;82:1-12.
3. Ocampo-Piraquive V, Nieto-Aristizábal I, Cañas CA, Tobón GJ. Mortality in systemic lupus erythematosus: causes, predictors and interventions. Expert Rev Clin Immunol. 2018;14(12):1043-53.
4. Sella EM, Sato EI, Barbieri A. Coronary artery angiography in systemic lupus erythematosus patients with abnormal myocardial perfusion scintigraphy. Arthritis Rheum. 2003;48(11):3168-75.
5. June RR, Scalzi LV. Peripheral vascular disease in systemic lupus patients. J Clin Rheumatol. 2013;19(7):367-72.
6. Alexánderson E, Ochoa JM, Calleja R, Juárez-Rojas JG, Prior JO, Jácome R, et al. Endothelial dysfunction in systemic lupus erythematosus: evaluation with 13N-ammonia PET. J Nucl Med. 2010;51(12):1927-31.
7. Rajagopalan S, Somers EC, Brook RD, Kehrer C, Pfenninger D, Lewis E, et al. Endothelial cell apoptosis in systemic lupus erythematosus: a common pathway for abnormal vascular function and thrombosis propensity. Blood. 2004;103(10):3677-83.
8. Gustafsson JT, Svenungsson E. Definitions of and contributions to cardiovascular disease in systemic lupus erythematosus. Autoimmunity. 2014;47(2):67-76.
9. Sun W, Jiao Y, Cui B, Gao X, Xia Y, Zhao Y. Immune complexes activate human endothelium involving the cell-signaling HMGB1-RAGE axis in the pathogenesis of lupus vasculitis. Lab Invest. 2013;93(6):626-38.
10. Tektonidou MG, Kravvariti E, Konstantonis G, Tentolouris N, Sfikakis PP, Protogerou A. Subclinical atherosclerosis in Systemic Lupus Erythematosus: Comparable risk with Diabetes Mellitus and Rheumatoid Arthritis. Autoimmun Rev. 2017;16(3):308-12.
11. Lewandowski LB, Kaplan MJ. Update on cardiovascular disease in lupus. Curr Opin Rheumatol. 2016;28(5):468-76.
12. Stojan G, Petri M. Epidemiology of systemic lupus erythematosus: an update. Curr Opin Rheumatol. 2018;30(2):144-50.
13. Ryan MJ, McLemore GR. Hypertension and impaired vascular function in a female mouse model of systemic lupus erythematosus. Am J Physiol Regul Integr Comp Physiol. 2007;292(2):R736-42.
14. Gomez-Guzman M, Jimenez R, Romero M, Sanchez M, Jose Zarzuelo M, Gomez-Morales M, et al. Chronic Hydroxychloroquine Improves Endothelial Dysfunction and Protects Kidney in a Mouse Model of Systemic Lupus Erythematosus. Hypertension. 2014;64(2):330-+.
15. Romero M, Toral M, Robles-Vera I, Sánchez M, Jiménez R, O'Valle F, et al. Activation of Peroxisome Proliferator Activator Receptor β/δ Improves Endothelial Dysfunction and Protects Kidney in Murine Lupus. Hypertension. 2017;69(4):641-50.
16. Chen JQ, Szodoray P, Zeher M. Toll-Like Receptor Pathways in Autoimmune Diseases. Clin Rev Allergy Immunol. 2016;50(1):1-17.

17. Wu YW, Tang W, Zuo JP. Toll-like receptors: potential targets for lupus treatment. Acta Pharmacol Sin. 2015;36(12):1395-407.
18. Weidenbusch M, Kulkarni OP, Anders HJ. The innate immune system in human systemic lupus erythematosus. Clin Sci (Lond). 2017;131(8):625-34.
19. Clancy RM, Markham AJ, Buyon JP. Endosomal Toll-like receptors in clinically overt and silent autoimmunity. Immunol Rev. 2016;269(1):76-84.
20. Murayama G, Furusawa N, Chiba A, Yamaji K, Tamura N, Miyake S. Enhanced IFN-α production is associated with increased TLR7 retention in the lysosomes of palasmacytoid dendritic cells in systemic lupus erythematosus. Arthritis Res Ther. 2017;19(1):234.
21. Nickerson KM, Christensen SR, Shupe J, Kashgarian M, Kim D, Elkon K, et al. TLR9 regulates TLR7- and MyD88-dependent autoantibody production and disease in a murine model of lupus. J Immunol. 2010;184(4):1840-8.
22. Liu Y, Seto NL, Carmona-Rivera C, Kaplan MJ. Accelerated model of lupus autoimmunity and vasculopathy driven by toll-like receptor 7/9 imbalance. Lupus Sci Med. 2018;5(1):e000259.
23. Yokogawa M, Takaishi M, Nakajima K, Kamijima R, Fujimoto C, Kataoka S, et al. Epicutaneous application of toll-like receptor 7 agonists leads to systemic autoimmunity in wild-type mice: a new model of systemic Lupus erythematosus. Arthritis Rheumatol. 2014;66(3):694-706.
24. Bolland S, Yim YS, Tus K, Wakeland EK, Ravetch JV. Genetic modifiers of systemic lupus erythematosus in FcgammaRIIB(-/-) mice. J Exp Med. 2002;195(9):1167-74.
25. Deane JA, Pisitkun P, Barrett RS, Feigenbaum L, Town T, Ward JM, et al. Control of toll-like receptor 7 expression is essential to restrict autoimmunity and dendritic cell proliferation. Immunity. 2007;27(5):801-10.
26. Fernandes DC, Wosniak J, Pescatore LA, Bertoline MA, Liberman M, Laurindo FR, et al. Analysis of DHE-derived oxidation products by HPLC in the assessment of superoxide production and NADPH oxidase activity in vascular systems. Am J Physiol Cell Physiol. 2007;292(1):C413-22.
27. Castro MM, Rizzi E, Rodrigues GJ, Ceron CS, Bendhack LM, Gerlach RF, et al. Antioxidant treatment reduces matrix metalloproteinase-2-induced vascular changes in renovascular hypertension. Free Radic Biol Med. 2009;46(9):1298-307.
28. Wang ZL, Luo XF, Li MT, Xu D, Zhou S, Chen HZ, et al. Resveratrol possesses protective effects in a pristane-induced lupus mouse model. PLoS One. 2014;9(12):e114792.
29. Quesada A, Vargas F, Montoro-Molina S, O'Valle F, Rodríguez-Martínez MD, Osuna A, et al. Urinary aminopeptidase activities as early and predictive biomarkers of renal dysfunction in cisplatin-treated rats. PLoS One. 2012;7(7):e40402.
30. Zarzuelo MJ, Jiménez R, Galindo P, Sánchez M, Nieto A, Romero M, et al. Antihypertensive effects of peroxisome proliferator-activated receptor-β activation in spontaneously hypertensive rats. Hypertension. 2011;58(4):733-43.
31. Nagata S, Hanayama R, Kawane K. Autoimmunity and the clearance of dead cells. Cell. 2010;140(5):619-30.
32. Sakamoto K, Fukushima Y, Ito K, Matsuda M, Nagata S, Minato N, et al. Osteopontin in Spontaneous Germinal Centers Inhibits Apoptotic Cell

Engulfment and Promotes Anti-Nuclear Antibody Production in Lupus-Prone Mice. J Immunol. 2016;197(6):2177-86.
33. Armbrust T, Nordmann B, Kreissig M, Ramadori G. C1Q synthesis by tissue mononuclear phagocytes from normal and from damaged rat liver: up-regulation by dexamethasone, down-regulation by interferon gamma, and lipopolysaccharide. Hepatology. 1997;26(1):98-106.
34. Ren D, Liu F, Dong G, You M, Ji J, Huang Y, et al. Activation of TLR7 increases CCND3 expression via the downregulation of miR-15b in B cells of systemic lupus erythematosus. Cell Mol Immunol. 2016;13(6):764-75.
35. Schiffrin EL. Remodeling of resistance arteries in essential hypertension and effects of antihypertensive treatment. Am J Hypertens. 2004;17(12 Pt 1):1192-200.
36. Briones AM, Rodríguez-Criado N, Hernanz R, García-Redondo AB, Rodrigues-Díez RR, Alonso MJ, et al. Atorvastatin prevents angiotensin II-induced vascular remodeling and oxidative stress. Hypertension. 2009;54(1):142-9.
37. Mak A, Kow NY, Schwarz H, Gong L, Tay SH, Ling LH. Endothelial dysfunction in systemic lupus erythematosus - a case-control study and an updated meta-analysis and meta-regression. Sci Rep. 2017;7(1):7320.
38. García-Redondo AB, Aguado A, Briones AM, Salaices M. NADPH oxidases and vascular remodeling in cardiovascular diseases. Pharmacol Res. 2016;114:110-20.
39. Tselios K, Gladman DD, Urowitz MB. Systemic lupus erythematosus and pulmonary arterial hypertension: links, risks, and management strategies. Open Access Rheumatol. 2017;9:1-9.
40. Lee YH, Choi SJ, Ji JD, Song GG. Association between toll-like receptor polymorphisms and systemic lupus erythematosus: a meta-analysis update. Lupus. 2016;25(6):593-601.
41. Chasset F, Arnaud L. Targeting interferons and their pathways in systemic lupus erythematosus. Autoimmun Rev. 2018;17(1):44-52.
42. Gong L, Wang Y, Zhou L, Bai X, Wu S, Zhu F, et al. Activation of toll-like receptor-7 exacerbates lupus nephritis by modulating regulatory T cells. Am J Nephrol. 2014;40(4):325-44.
43. Botto M, Walport MJ. C1q, autoimmunity and apoptosis. Immunobiology. 2002;205(4-5):395-406.
44. Crispín JC, Hedrich CM, Tsokos GC. Gene-function studies in systemic lupus erythematosus. Nat Rev Rheumatol. 2013;9(8):476-84.
45. Spolski R, Leonard WJ. Interleukin-21: a double-edged sword with therapeutic potential. Nat Rev Drug Discov. 2014;13(5):379-95.
46. Taylor EB, Ryan MJ. Understanding mechanisms of hypertension in systemic lupus erythematosus. Ther Adv Cardiovasc Dis. 2016.
47. Venegas-Pont M, Manigrasso MB, Grifoni SC, LaMarca BB, Maric C, Racusen LC, et al. Tumor necrosis factor-alpha antagonist etanercept decreases blood pressure and protects the kidney in a mouse model of systemic lupus erythematosus. Hypertension. 2010;56(4):643-9.
48. Taylor EB, Ryan MJ. Immunosuppression With Mycophenolate Mofetil Attenuates Hypertension in an Experimental Model of Autoimmune Disease. J Am Heart Assoc. 2017;6(3).

49. Sabio JM, Vargas-Hitos JA, Martínez-Bordonado J, Navarrete-Navarrete N, Díaz-Chamorro A, Olvera-Porcel C, et al. Cumulated organ damage is associated with arterial stiffness in women with systemic lupus erythematosus irrespective of renal function. Clin Exp Rheumatol. 2016;34(1):53-7.
50. Rudofsky UH, Dilwith RL, Roths JB, Lawrence DA, Kelley VE, Magro AM. Differences in the occurrence of hypertension among (NZB X NZW)F1, MRL-lpr, and BXSB mice with lupus nephritis. Am J Pathol. 1984;116(1):107-14.
51. Schiffrin EL. Vascular remodeling in hypertension: mechanisms and treatment. Hypertension. 2012;59(2):367-74.
52. Laurent S, Boutouyrie P. The structural factor of hypertension: large and small artery alterations. Circ Res. 2015;116(6):1007-21.
53. Touyz RM, Briones AM. Reactive oxygen species and vascular biology: implications in human hypertension. Hypertens Res. 2011;34(1):5-14.
54. El-Magadmi M, Bodill H, Ahmad Y, Durrington PN, Mackness M, Walker M, et al. Systemic lupus erythematosus: an independent risk factor for endothelial dysfunction in women. Circulation. 2004;110(4):399-404.
55. Kofler S, Nickel T, Weis M. Role of cytokines in cardiovascular diseases: a focus on endothelial responses to inflammation. Clin Sci (Lond). 2005;108(3):205-13.
56. Small HY, Migliarino S, Czesnikiewicz-Guzik M, Guzik TJ. Hypertension: Focus on autoimmunity and oxidative stress. Free Radic Biol Med. 2018;125:104-15.
57. Buie JJ, Renaud LL, Muise-Helmericks R, Oates JC. IFN-α Negatively Regulates the Expression of Endothelial Nitric Oxide Synthase and Nitric Oxide Production: Implications for Systemic Lupus Erythematosus. J Immunol. 2017;199(6):1979-88.
58. Chen JX, Stinnett A. Critical role of the NADPH oxidase subunit p47phox on vascular TLR expression and neointimal lesion formation in high-fat diet-induced obesity. Lab Invest. 2008;88(12):1316-28.
59. De Meyer I, Martinet W, Schrijvers DM, Timmermans JP, Bult H, De Meyer GR. Toll-like receptor 7 stimulation by imiquimod induces macrophage autophagy and inflammation in atherosclerotic plaques. Basic Res Cardiol. 2012;107(3):269.
60. Komai T, Inoue M, Okamura T, Morita K, Iwasaki Y, Sumitomo S, et al. Transforming Growth Factor-β and Interleukin-10 Synergistically Regulate Humoral Immunity. Front Immunol. 2018;9:1364.
61. Li W, Li Q, Jiao Y, Qin L, Ali R, Zhou J, et al. Tgfbr2 disruption in postnatal smooth muscle impairs aortic wall homeostasis. J Clin Invest. 2014;124(2):755-67.

TABLES

Table 1. Morphological parameters.

Variables	Ctrl 4W (n=8)	IMQ 4W (n=8)	Ctrl 8W (n=8)	IMQ 8W (n=8)
BW (g)	21.54±0.61	21.75±0.64	21.89±0.54	24.10± 0.62 ** †
TL (mm	20.61±0.19	21.50±0.40	21.11±0.14	21.13± 0.30
HW/TL (mg/cm)	4.56±0.16	4.71±0.14	4.61±0.11	5.25± 0.24 * †
LVW/TL (mg/cm)	2.93±0.07	2.91±0.08	2.80±0.06	3.17± 0.12 * †
KW/TL (mg/cm)	5.36±0.06	5.89±0.21 *	5.20±0.08	6.83± 0.43 ** †
LW/TL (mg/cm)	42.35±2.49	67.15±2.29 **	39.29±1.42	86.26± 5.88 ** ††
Spleen/TL (mg/cm)	4.50±0.17	24.04±2.00 **	4.70±0.29	36.18± 3.63 ** †
Mesenteric fat/BW (%)	0.42±0.03	0.39±0.04	0.38±0.02	0.21±0.03 ** ††
Gonadal fat/BW (%)	2.04±0.18	1.89±0.18	1.80±0.16	0.89±0.07 ** ††

Results are shown as mean ± SEM. *P < 0.05 and **P < 0.01 vs control gruop; †P < 0.05 and † † P < 0.01 vs IMQ 4 weeks group. BW, Body weight; TL, Tibia length; HW, Heart weight; LVW, Left ventricular weight; KW, Kidney weight; LW, Liver weight.

FIGURE

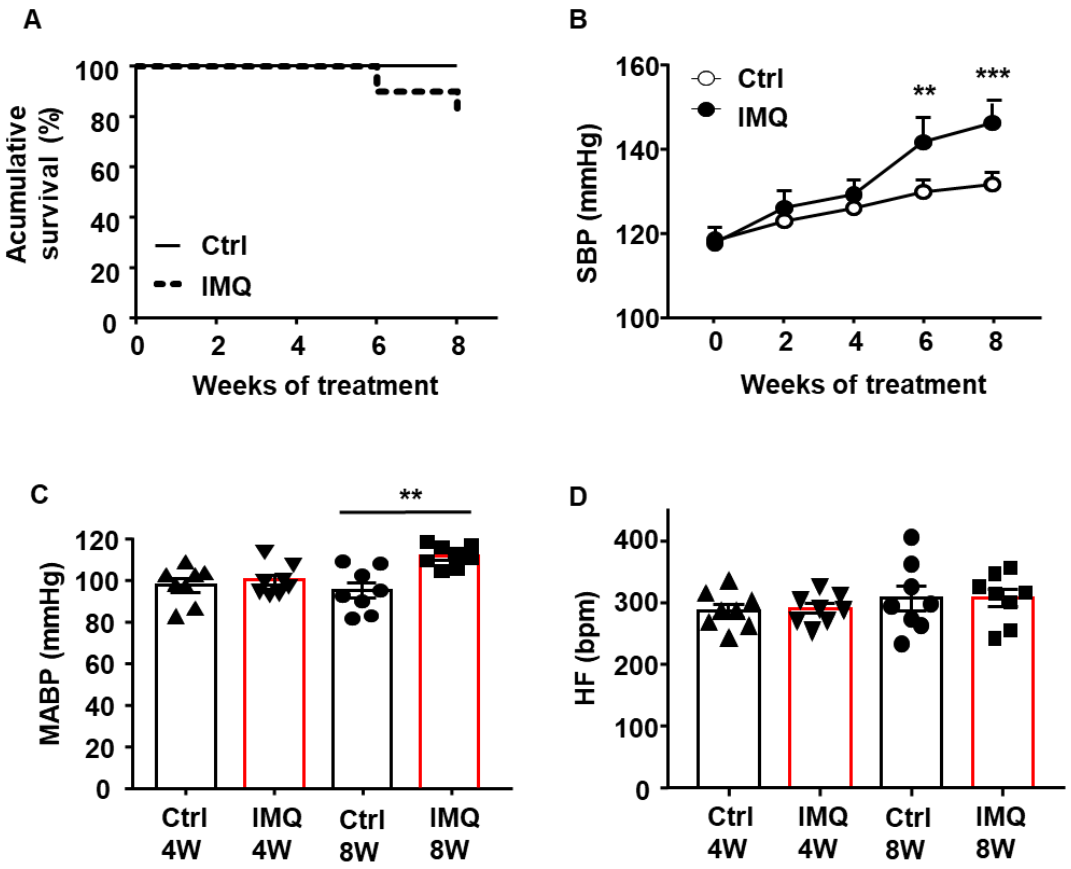

Figure 1. TLR7 activation promotes blood pressure increase in imiquimod-induced autoimmunity. (A) Cumulative survival rate of BALB/c mice following topical application of imiquimod (IMQ) on their right ears three times weekly during 8 weeks. (B) Time course of systolic blood pressure (SBP) measured by tail-cuff plethysmography was determined in control (Ctrl) and IMQ-treated mice. (C) Mean arterial blood pressure (MABP) and (D) heart rate (HR) measured by direct register in left carotid artery at the end of the experimental period. Experimental groups: Ctrl 4W (n=8), Ctrl 8W (n=8), IMQ 4W (n=8), IMQ 8W (n=8). Values are expressed as Mean ± SEM. Results were compared by 1-way ANOVA and Tukey post hoc test. **P<0.01, ***P<0.001 as compared to the control group.

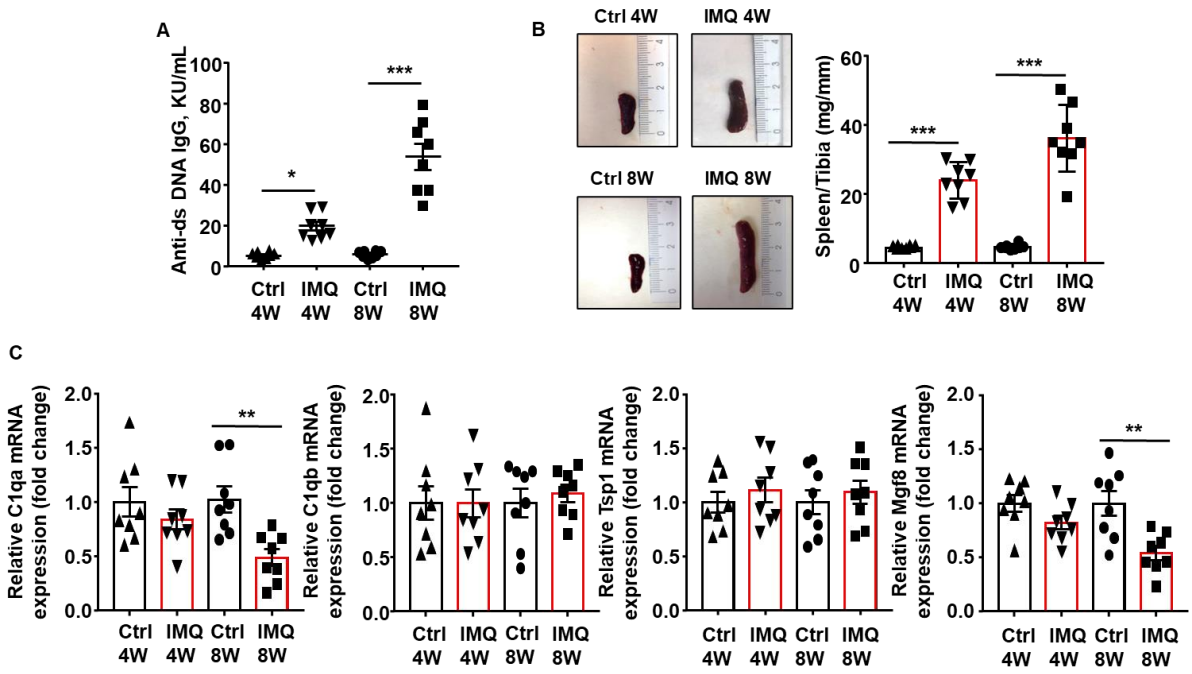

Figure 2. TLR7 activation leads to higher levels of serum autoantibodies anti-dsDNA, marked splenomegaly and altered clearance of apoptotic cells in imiquimod-treated mice. (A) Circulating double-stranded DNA autoantibodies, (B) splenomegaly, and (C) hepatic opsonins mRNA levels measured by reverse transcriptase-polymerase chain reaction, were assessed in control (Ctrl) and imiquimod (IMQ)-treated mice. Experimental groups: Ctrl 4W (n=8), Ctrl 8W (n=8), IMQ 4W (n=8), IMQ 8W (n=8). Results were compared by 1-way ANOVA and Tukey post hoc test. Values are expressed as Mean ± SEM. *P<0.05, **P<0.01, ***P<0.001 as compared to the control group.

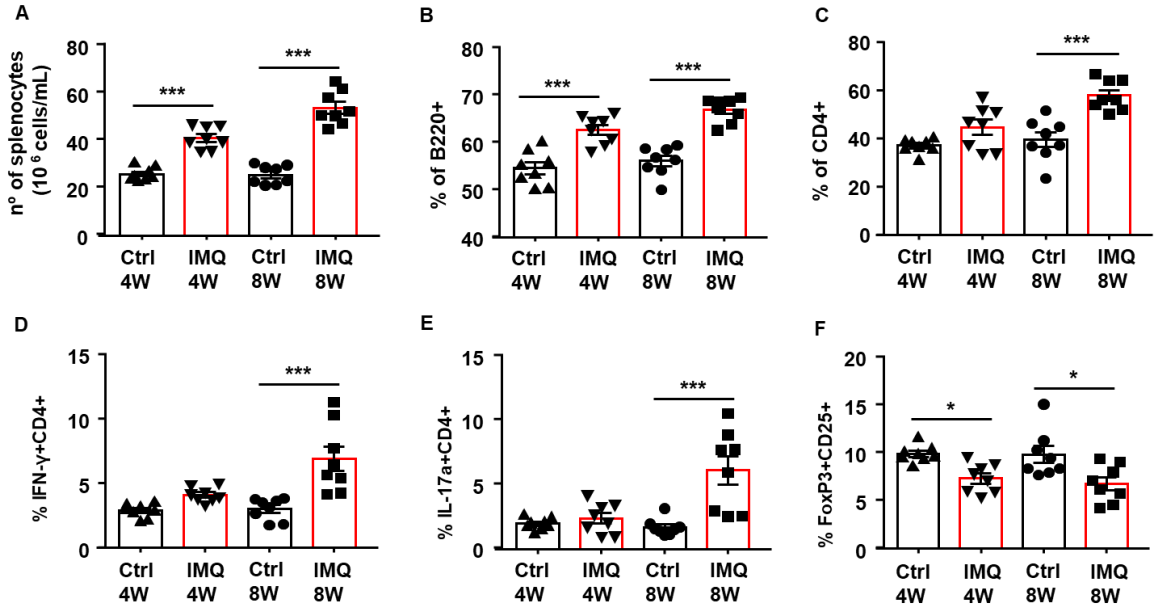

Figure 3. TLR7 activation induces splenic B cells and T cells increase and promotes T-cell polarization to proinflammatory phenotype. (A) Number of total cells, (B) percentage of B cells and (C) percentage of T cells were measured by flow cytometry in spleens from imiquimod (IMQ)-treated mice. (D) Percentage of Th1, (E) Th17 and (F) Treg cells measured by flow cytometry were assessed in control (Ctrl) and IMQ-treated mice. Experimental groups: Ctrl 4W (n=8), Ctrl 8W (n=8), IMQ 4W (n=8), IMQ 8W (n=8). Results were compared by 1-way ANOVA and Tukey post hoc test. Values are expressed as Mean ± SEM. *P<0.05, ***P<0.001 as compared to the control group.

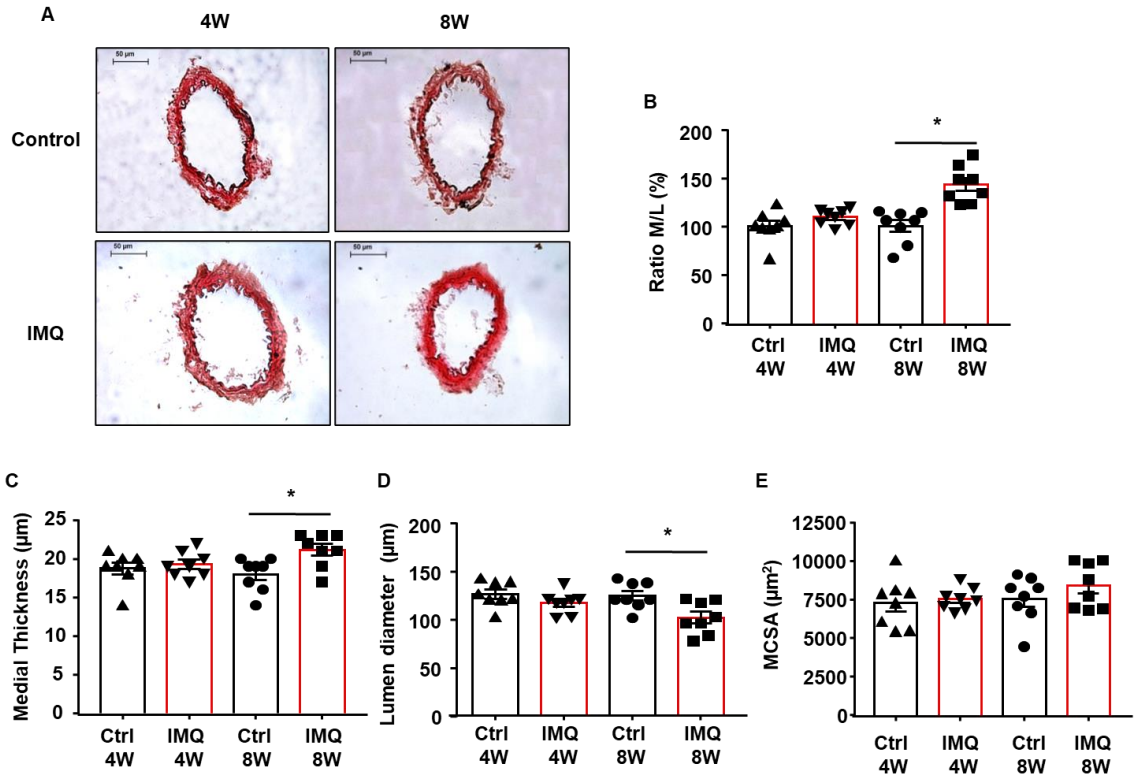

Figure 4. TLR7 activation promotes vascular remodeling in imiquimod-treated mice. Effects of TLR7 activation on structural modifications induced in superior mesenteric arteries from IMQ-treated mice. (A) Representative histological sections of paraffin-embedded tissues stained with hematoxylin-eosin. Morphometric analysis of media:lumen ratio (M/L) (B), medial thickness (C), lumen diameter (D) and media cross-sectional area (MCSA) (E). Experimental groups: Ctrl 4W (n=8), Ctrl 8W (n=8), IMQ 4W (n=8), IMQ 8W (n=8). Results were compared by 1-way ANOVA and Tukey post hoc test. Values are expressed as Mean ± SEM. *P<0.05 as compared to the control group.

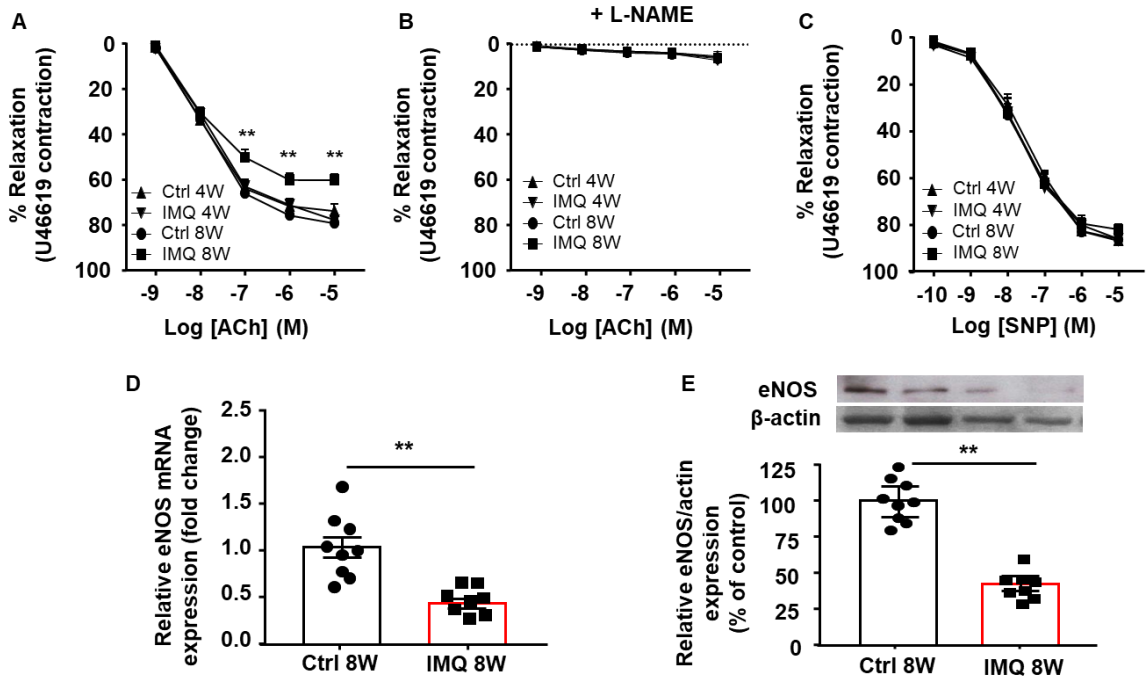

Figure 5. TLR7 activation leads to marked impairment of endothelium-dependent vasorelaxation in imiquimod-treated mice. Vascular relaxant responses induced by acetylcholine (ACh, 1nM–10µM), in endothelium-intact aortae pre-contracted by U46619 (10nM) in the absence (A) or in the presence of the endothelial NO synthase (eNOS) inhibitor N(ω)-nitro-L-arginine methyl ester (L-NAME, 100µM) (B). (C) Endothelium-independent relaxant responses to sodium nitroprusside (SNP, 0,1nM–10µM) in endothelium-denuded vessels pre-contracted by U46619 (10nM). Relaxant responses to Ach and SNP were expressed as a percentage of pre-contraction induced by U46619. (D) mRNA expression and (E) protein expression of eNOS in aorta homogenates from all experimental groups. Data are presented as a ratio of arbitrary units of mRNA ($2^{-\Delta\Delta Ct}$) or eNOS/actin ratio compared with control group. Experimental groups: Ctrl 4W (n=8), Ctrl 8W (n=8), IMQ 4W (n=8), IMQ 8W (n=8). Results

were compared by 1-way ANOVA and Tukey post hoc test. Values are expressed as Mean ± SEM. **P<0.01 as compared to the control group.

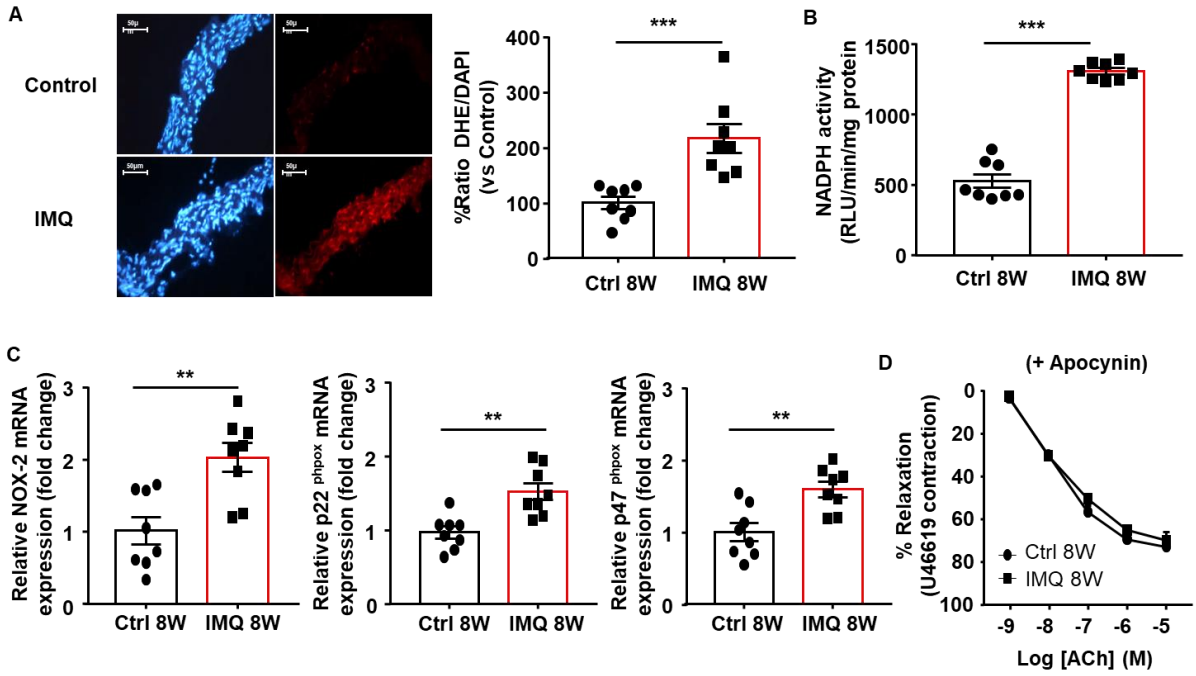

Figure 6. TLR7 activation promotes a significant increase on vascular reactive oxygen species and NADPH oxidase activity in aorta from imiquimod-treated mice. (A) Representative pictures of arteries incubated in the presence of dihydroethidium (DHE), which produces a red fluorescence when oxidized to ethidium by O_2^-, and the nuclear stain 4,6-diamidino-2-phenylindoledichlorohydrate (DAPI), which produces a blue fluorescence (magnification X400), and averaged values of the red ethidium fluorescence normalized to the blue DAPI fluorescence, mean±SEM (n= 8). (B) NADPH oxidase activity measured by lucigenin-enhanced chemiluminescence. (C) mRNA expression of NADPH oxidase subunits NOX-2, p22phox and p47phox in aorta homogenates from all experimental groups. Data are presented as a

ratio of arbitrary units of mRNA ($2^{-\Delta\Delta Ct}$). (D) Endothelium-dependent vasodilator responses to acetylcholine (ACh) in intact aortic rings precontracted with U46619 (10 nM) in the presence of apocynin (10 μM). Experimental groups: Ctrl 8W (n=8), IMQ 8W (n=8). Results were compared by 1-way ANOVA and Tukey post hoc test. Values are expressed as Mean ± SEM. **P<0.01 and ***P<0.001 as compared to the control group.

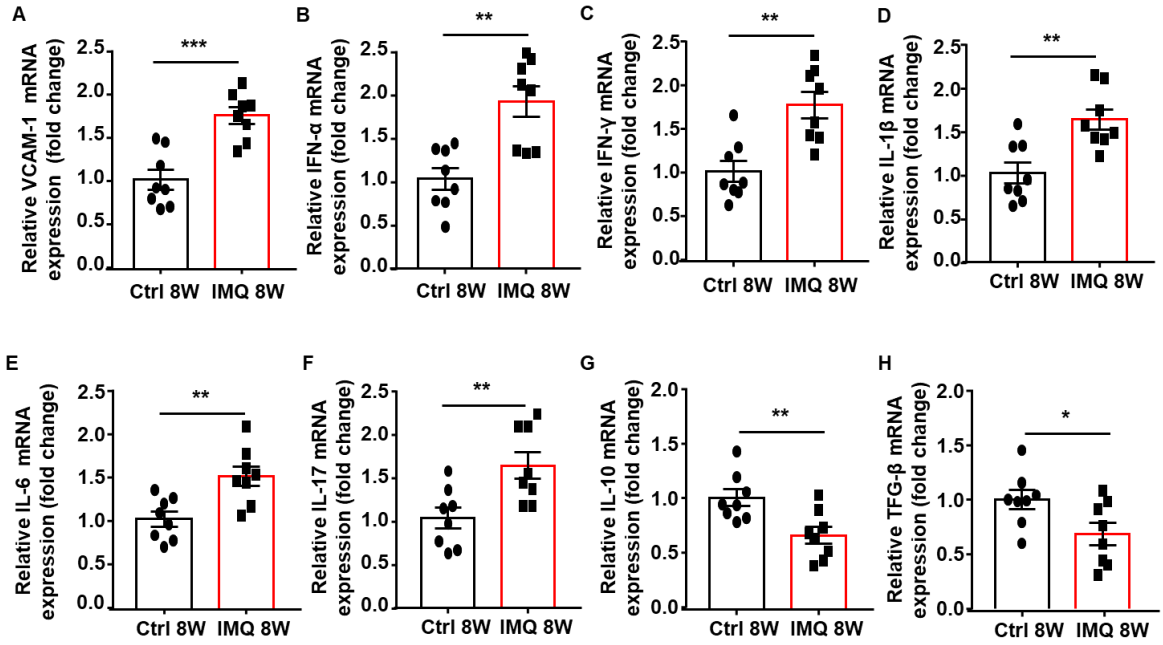

Figure 7. TLR7 activation promotes a higher gene expression of vascular adhesion molecules and proinflammatory cytokines in aorta from imiquimod-treated mice. mRNA expression of vascular cell adhesion molecule-1 (VCAM-1) (A), proinflammatory cytokines IFN-α (B), IFNγ (C), IL1β (D), IL-6 (E) and IL-17 (F), and anti-inflammatory cytokine IL-10 (G) and TFG-β (H) in aorta homogenates from IMQ-treated mice at 8 weeks of treatment. Data are presented as a ratio of arbitrary units of mRNA ($2^{-\Delta\Delta Ct}$). Experimental groups: Ctrl 8W (n=8), IMQ 8W (n=8). Results were compared by 1-way

ANOVA and Tukey post hoc test. Values are expressed as Mean ± SEM. *P<0.05, **P<0.01, ***P<0.001 as compared to the control group.

.